APPENDIX K

Memo on the Impact of Chronic Lowering of Water Levels in the ELPMA

605 THIRD STREET
ENCINITAS, CALIFORNIA 92024
T 760.942.5147 F 760.632.0164

MEMORANDUM

To: Kim Loeb, Fox Canyon Groundwater Management Agency
From: Peter Quinlan, Trevor Jones
Subject: Evaluating the Impact of Chronic Lowering of Water Levels on Storage, Recharge, and Well Yields in ELPMA
Date: May 10, 2019
cc: Ron Schnabel
Attachment(s):

1 Executive Summary

This memo describes work performed to evaluate potential undesirable results associated with chronic declines in water levels in the East Las Posas Management Area of the Las Posas Valley Basin (ELPMA). Using the 50-year simulation of future baseline conditions for the ELPMA, we evaluated potential changes in the amount of the groundwater in storage, potential changes in the production capacity of the Fox Canyon Aquifer (FCA), and potential impacts on recharge due to conversion of the Fox Canyon Aquifer from confined to unconfined conditions.

The evaluation used the numerical model prepared by Calleguas Municipal Water District. The model predicts that continued production at 22,000 AFY throughout the ELPMA (the average 2015-2017 rate) would result in an ELPMA-wide loss of more than 209,000 acre-feet (AF) of groundwater in storage. This is equivalent to approximately 8% of groundwater in storage in 2015. Approximately 90,000 AF of this loss occurs in the Upper San Pedro Formation which is the reservoir containing accumulated recharge from past centuries that leaks downward to replenish the Fox Canyon Aquifer. However, along the northern and southern basin margins and in the center of the basin along the Moorpark and Long Canyon Anticlines, the Fox Canyon Aquifer would experience reductions in storage ranging from 25% to 36%. Additionally, there is a 45% reduction in groundwater in storage in the Epworth Gravels aquifer.

ELPMA-wide 50-year declines in water levels would reduce the production capacity of the FCA by 3%, areas along the northern and southern basin margin and in the center of the basin along the Moorpark Anticline would experience production decreases of 56% to 78%.

As water levels decline in the FCA, the top of the FCA becomes unsaturated in some areas. Leakage from the overlying Upper San Pedro Formation is slightly impeded by unsaturated flow conditions and is reduced locally by approximately 10%. ELPMA-wide this reduction is estimated to amount to approximately 650 AFY.

Background

Calleguas Municipal Water District (CMWD) has developed a numerical groundwater model that reproduces historical trends in groundwater elevations across the East Las Posas Management Area of the Las Posas Valley Basin. To assess the future sustainable yield of the basin, Fox Canyon Groundwater Management Agency (FCGMA) contracted with CMWD to simulate several model scenarios developed by Dudek and FCGMA that varied groundwater production and assessed the efficacy of different projects to mitigate the impact of reduced recharge into the groundwater basin under future climate scenarios.

The Future Baseline Simulation provides estimates of basin-wide groundwater elevation changes under recent production conditions and current basin-management strategies. In this scenario, 22,000 AF of groundwater is extracted from the basin annually, discharges to Arroyo Las Posas by the City of Simi Valley are reduced by up to approximately 5,200 AFY, and no new projects are implemented.

Groundwater elevation hydrographs analyzed from the future baseline model scenario demonstrate declines throughout the simulation. The continued decline in groundwater levels at these discrete locations suggest a reduction in basin-wide storage and potential negative impacts to well yields across the ELPMA.

To assess basin-wide metrics under the Future Baseline Scenario conditions, we performed additional analyses using the model outputs to quantify changes in groundwater elevations, storage, and well yields across the entire model domain throughout the 50-year simulation period. The storage and groundwater elevation estimates were compared to aquifer states in December 2015 and December 1974 when groundwater elevations in the vicinity of Arroyo Las Posas were are at historical low levels. Below we describe our approach to quantifying basin-wide groundwater elevation changes, reduction in storage, and losses in well productivity. After describing the methods for each approach, we present results from the analysis at the basin- and local-scale.

Methods

Change in groundwater elevations across the domain

The numerical groundwater model developed by CMWD provides estimates of groundwater head at discrete locations across the Epworth Gravels, Shallow Aquifer, Upper San Pedro (USP), regional clay marker bed, Fox Canyon Aquifer (FCA), Upper Santa Barbara Formation, and Grimes Canyon Aquifer (GCA). These estimates correspond to the center of each computational cell in the model and occur at a spatial resolution of 200 by 200 ft. The composite matrix of discrete head values provides a quantitative description of the head distribution within each model layer for each of the 600 monthly stress periods in the Future Baseline Scenario simulation.

To calculate the change in groundwater elevation between two time periods, we take the difference between head field matrices at discrete times in the simulations:

$$\Delta H^m_{i,j,k} = H^n_{i,j,k} - H^m_{i,j,k} \qquad (1)$$

Where:

n is the stress period of interest

m is the reference stress period

i is the model row

j *is the model column*

and

k is the model layer, which is associated with a unique stratigraphic unit

Here, negative ΔH values denote locations where groundwater elevations have declined since the reference period *m*, and positive ΔH values denote locations where groundwater heads have increased since reference period *m*.

Estimates of aquifer storage

Estimates of groundwater head in each model cell provide the ability to directly quantify the total volume of water stored in each model layer throughout the simulation. As the net flux into a model cell increases, fluid is continuously stored in the pore-spaces of the rock matrix due to either progressive filling of the partially saturated cell or expansion of the rock-fluid matrix. The capacity of any given cell to store water is given by the local storativity, *S*:

$$S = S_y + bS_s \quad (2)$$

Where:

S_y is the specific yield [-]

S_s is the specific storage of the material [1/L]

and

b is the saturated thickness of the cell [L]

Sy describes the ability for water to drain or fill the local pore-spaces in an unconfined aquifer, and Ss describes the capacity of a local representative volume to store/release water due to the expansion and contraction of the matrix.

The relationship between the volume of stored water, head, and storativity, *S*, is given by Fetter (2001):

$$\frac{dV_w}{dh} = SA \qquad (3)$$

Equation (3) provides a direct relationship between the volume of water released from a porous medium with cross-sectional area, A, that has storativity, S, due to a unit change in head. Integrating (3) from the top elevation of the water surface to the bottom elevation of the cell provides an estimate of the total water stored in each cell.

Delineation between Confined and Unconfined Storage: Simplifying Assumptions and Method of Integration

Changes in storage under unconfined conditions are driven by two mechanisms: (i) the draining and filling of void spaces in the medium, and (ii) the compression and expansion of the fluid-rock matrix as pore-pressures fluctuate. As previously mentioned, changes in storage via mechanism (i) are represented through the coefficient *Sy*. In the numerical model developed by CMWD, the smallest value of Sy used in principal aquifer units was 0.15; values of Sy = 0.15 occur in the FCA and the USP. In cells that are characterized by this relatively low specific yield, the corresponding specific storage coefficients, Ss, range from 5×10^{-5} to 1×10^{-4} ft^{-1}. Because Ss is much smaller than Sy across the model domain, we assume that draining/filling processes are the dominant source of storage changes; as a result, we neglect the influence of matrix compressibility when integrating (3) in cells that are unconfined.

The previous assumption allows us to separate storage in a given cell into two primary components: (1) confined storage, and (2) unconfined storage. When a cell is confined, storage changes are driven by the compression/expansion of the fluid-rock matrix. To quantify the total storage that occurs under confined conditions, we integrate (3) from the top elevation of the water surface (given by the head in that cell) to the top elevation of the cell. The discrete form of this integral is given by:

$$V_{w,conf}^{n} = S_s bA * (H_{i,j,k}^{n} - Z_{i,j,k}^{top}) \qquad (4)$$

Here $Z_{i,j,k}^{top}$ is the top elevation of the cell located at (*i*,*j*,*k*). After the water level drops below the top of the cell, gravity drainage becomes the dominant storage mechanism, and we treat the cell as if it were unconfined. To estimate the total volume of water in drainable storage after the cell becomes unconfined, we integrate (3) across the entire thickness of the cell:

$$V_{w,drain} = S_y A * \left(Z_{i,j,k}^{top} - Z_{i,j,k}^{bot}\right) \qquad (5)$$

Here $Z_{i,j,k}^{bot}$ is the bottom elevation of the cell located at (i,j,k). Note that (5) is a time-independent expression because it is defined solely by the geometric properties of the model cell. The total volume of water stored in a cell that occurs under confined conditions is given by the sum of (4) and (5).

Estimates of storage in a cell that is originally unconfined are calculated using an approach similar to (5). However, because the saturated thickness of the cell now depends on the head in the cell, the bounds of integration change. To adjust for this, we integrate (3) from the water table surface to the bottom of the cell, which takes the form of:

$$V_{w,unconfined}^{n} = S_y A * \left(H_{i,j,k}^{n} - Z_{i,j,k}^{bot}\right) \qquad (6)$$

To calculate the total volume of water stored in each model layer, we first segregate the domain into confined/unconfined cells and calculate the local storage using (4) and (5), or (6). In cells that are initially unsaturated ($H_{i,j,k}^{n} < Z_{i,j,k}^{bot}$), we set storage equal to 0. After calculating storage for each model cell, we sum the storage estimates across the model domain to generate global estimates of storage for each of the principal aquifer units.

Approach for Simulating Reduced Aquifer Productivity

Declining water levels potentially impact well yields by causing a transition between confined and unconfined conditions in the FCA, which is the primary production unit in East Las Posas. As regions of high productivity transition from confined to unconfined, well yields will decrease due to a decreasing saturated thickness of the aquifer (Konikow et. al, 2009). The numerical model developed by CMWD does not incorporate the effect of decreasing saturated thickness on well yields.

MODFLOW's NWT solver provides the ability to simulate decreasing well productivity as the saturated thickness of the cell decreases (Niswonger et. al, 2011). This approach uses an analytical expression for well production as a function of saturated thickness (see pg. 14 in Niswonger et. al (2011) for equations), and monotonically decreases the well yield as a cell progressively dries. This approach is dependent on the user-specified parameter, Φ, which controls the saturated thickness at which well yields begin to reduce. Figure 1 shows how Φ controls the reduction in well yield as the saturated thickness of the cell decreases. To provide a conservative estimate for reductions in well yield, we reran the Future Baseline Scenario using Φ = 0.99. The results of this simulation are presented in the section discussing reductions in well yields.

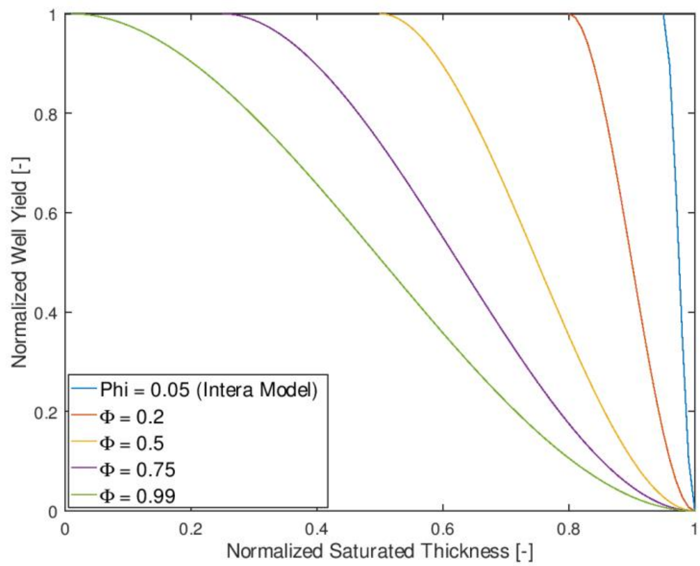

Figure 1: MODFLOW's approach to reducing well yield using the WEL package

Delineation between Eastern and Western Portions of the Model

Groundwater elevations in the eastern extent of the model domain show a monotonic increase throughout the Future Baseline Scenario simulation. In this eastern portion of the model (see Figure 2), the USP, FCA, and GCA progressively thin and are recharged via relatively large recharge rates (up to 30-inches per year) estimated by the Basin Characteristics Model (BCM) prepared for the vicinity of the Las Posas Valley Basin by the United States Geological Survey. The model-simulated increase in head is in contrast to the groundwater elevation declines that occur in the western portion of the model, where production occurs and the aquifer properties are constrained by measured data.

Storage in the eastern portion of the domain is a small fraction of the total volume of water stored in each of the principal aquifers. In the FCA, this eastern segment contained 20,100 AF of water based on simulated Dec 2015 conditions (2% of the total FCA storage). Similarly, in the USP, only 4% of the total storage occurs in the eastern portion of the model domain. Throughout the predictive simulation, the flux of water from the eastern to western section of the model averaged between 107 and 207 AFY for the USP and FCA, respectively – this is less than 1% of the total flux into the USP and FCA. In the GCA, storage and recharge from the east is more significant: storage in the eastern portion of the domain comprised approximately 14% of the total storage in the GCA, and the flux from the east averaged 1980 AFY. This accounted for 34% of the total flux into the western portion of the GCA.

The lack of measured data, and application of unconstrained BCM-estimated recharge rates, in this region limits quantitative calibration in the eastern section of the model. This increases uncertainty in model predictions east of the FCGMA boundary. Further, because increasing heads in the eastern portion of the model mask storage declines in the west where production occurs, we neglect the eastern portion of the model in our analysis.

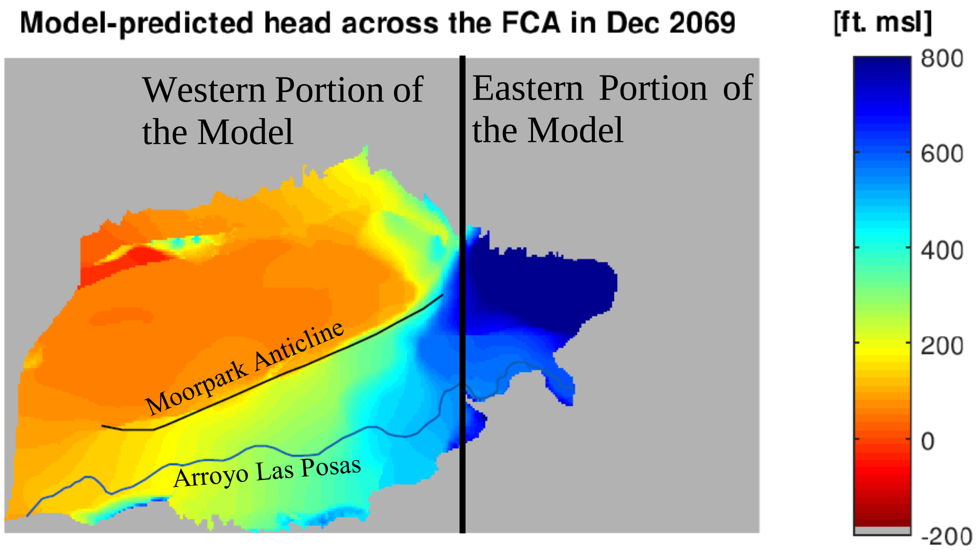

Figure 2: Model-predicted head distribution in Dec 2069. Eastern portion of the model shows anomalously high groundwater elevations that increase throughout the Future Baseline Scenario simulation.

Results

Groundwater production occurs predominantly in the Fox Canyon Aquifer, which is recharged via precipitation along the outcrop, and through leakage across regional confining beds that separate the FCA from the GCA and USP. Declining heads in the USP and Grimes may negatively impact recharge rates to the FCA. The interconnected nature of these primary units points to the need to assess groundwater elevation changes in the USP, the FCA, and the GCA. Below we present results for groundwater elevation changes and storage losses in each unit. Because the USP is separated into two layers within the model, we consider layers 2 and 3 of the model (both the USP) as separate units. When discussing groundwater elevation declines we focus on Layer 3 of the USP; we incorporate results from both layers when quantifying storage in the USP.

Declining Groundwater Elevations under Future Baseline Scenario Conditions

Groundwater elevations in the USP are largely influenced by areal recharge and discharge to the Arroyo Simi/Arroyo Las Posas. Under Future Baseline Scenario conditions, discharge to the Arroyo is decreased by up to 5,200 AFY by 2040, which results in less focused recharge to the USP. Figure 3 shows that reduced recharge along the Arroyo leads to a decline in groundwater elevations of over 100 feet in the southern portion of the domain by Dec 2069. In the eastern portion of the USP, south of the Moorpark anticline, groundwater elevations are similar to conditions in Dec 2015. North of the Moorpark anticline, groundwater elevations drop nearly 80 feet, and at the base of the South Mountain and Oak Ridge Mountains, groundwater elevations decline by more than 200 feet.

Reduced recharge to the USP impacts groundwater elevations in the Fox when production is maintained at 22,000 AFY across the basin (Figure 4). Basin production under these conditions leads to a wide-spread decline in groundwater elevations upwards of 100 feet across the western portion of the domain. In the southwestern portion of the FCA, groundwater elevation declines are largest underlying the Arroyo. In the southeastern portion of the domain, groundwater elevations remain similar to those predicted by the numerical model in Dec 2015. However, northwest of the anticline, groundwater heads drop by as much as 90 feet. Declines in head occur to a lesser extent in the north-eastern corner of the domain, which is likely influenced by recharge from the GCA that originates from the Happy Camp Area.

Groundwater elevation changes in the GCA are similar to those in the FCA. Groundwater elevation declines are largest in the western portion of the FCA, and drop by more than 200-feet north of the Long Canyon Syncline. In the northeastern portion of the domain, groundwater elevations increase due to recharge directly into the Grimes from the outcrop in the Happy Camp area.

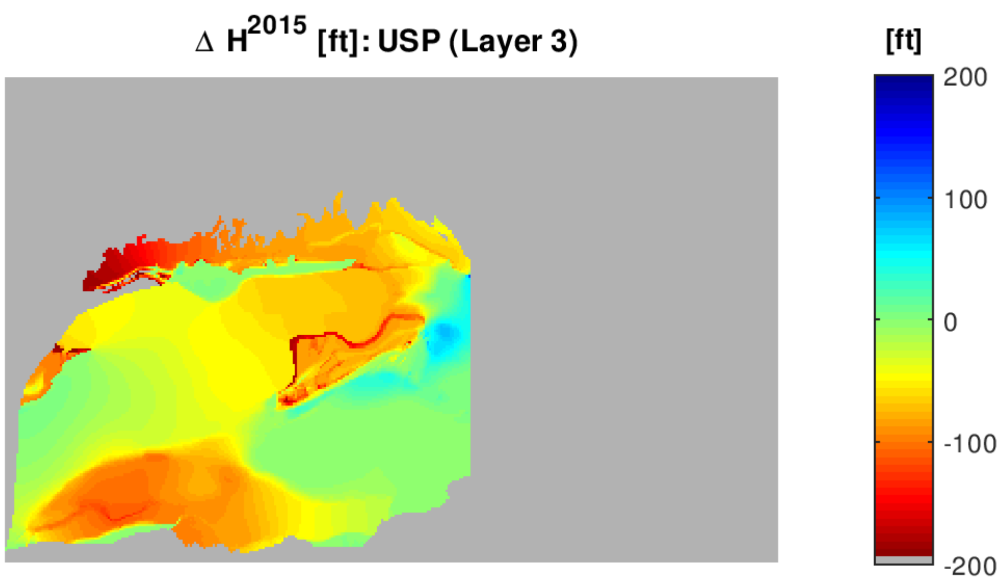

Figure 3: Changes in groundwater head in the USP (Layer 3) between Dec 2015 and Dec 2069.

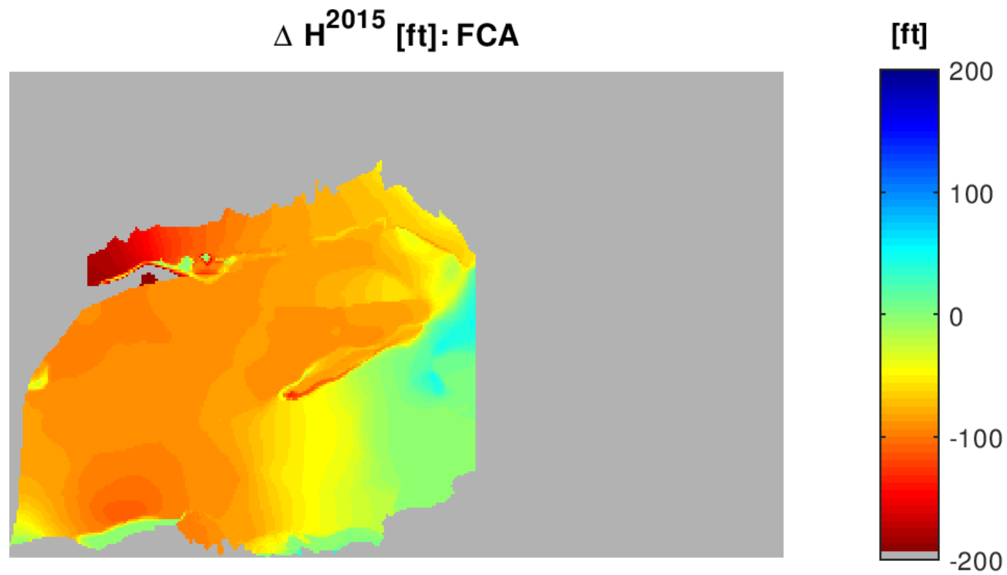

Figure 5: Changes in groundwater elevations in the FCA between Dec 2015 and Dec 2069

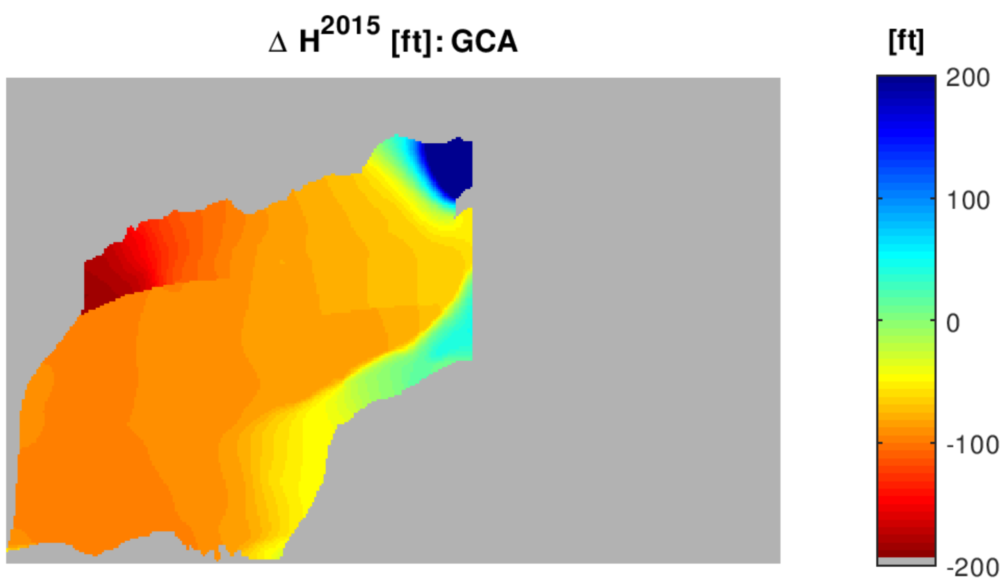

Figure 4: Changes in groundwater elevation in the GCA between Dec 2015 and Dec 2069.

Comparison between Simulated Water Levels in Dec 1974 and Predicted Water Levels in Dec 2069

The comparison between predicted Dec 2069 and Dec 2015 water levels show that groundwater elevations decline to the largest extent in the FCA and GCA. These declines are largest north of the Long Canyon Syncline and in the southwestern portion of the domain, where groundwater levels dropped by more than 100 feet. To provide further context for these predicted December 2069 groundwater elevations, we compared groundwater elevations from the end of the Future Baseline Scenario simulation to water levels predicted from the CMWD numerical model in December 1974.

Figures 6, 7, and 8 show the change in groundwater elevations in the USP (Layer 3), FCA, and GCA, respectively. The results from these figures show that groundwater elevations in Dec 2069 are lower than Dec 1974 water levels northwest of the Moorpark anticline. These declines are greatest in the USP, where groundwater elevations are lower than 1974 levels by more than 250 feet. In each aquifer unit, groundwater elevations decline by over 200 feet along the base of South Mountain. In the FCA and GCA, groundwater elevations decline by approximately 150 feet northwest of the Moorpark anticline. Southeast of the anticline and in the western portion of the domain, the simulation results show that groundwater elevations are higher in Dec 2069 than in 1974. This difference is largest in the vicinity of Arroyo Simi/Arroyo Las Posas, which indicates that increased storage via focused recharge along the creek had not been depleted by the end of the 2069 simulation.

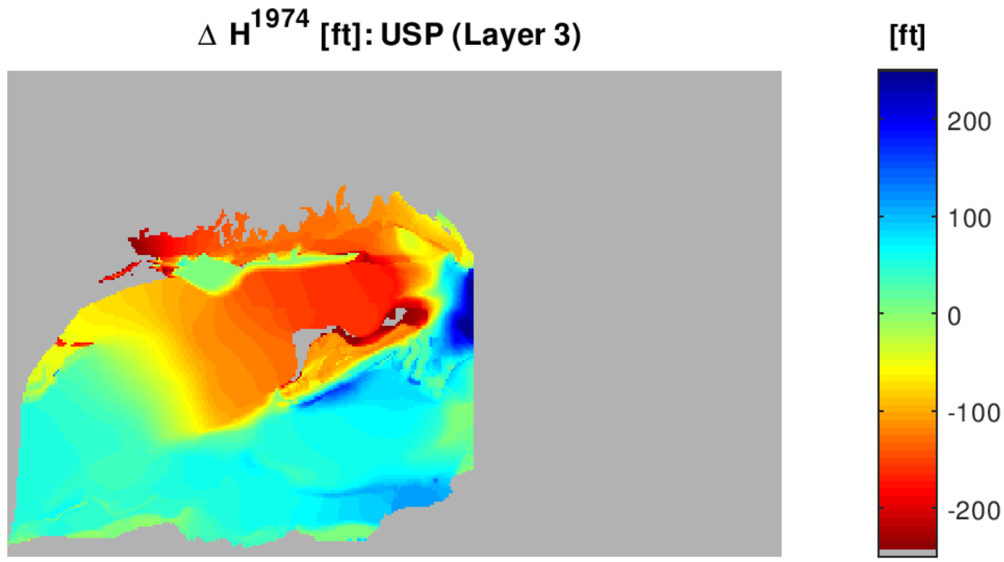

Figure 6: Difference in groundwater elevation in the USP (layer 3) between Dec 1974 and Dec 2069.

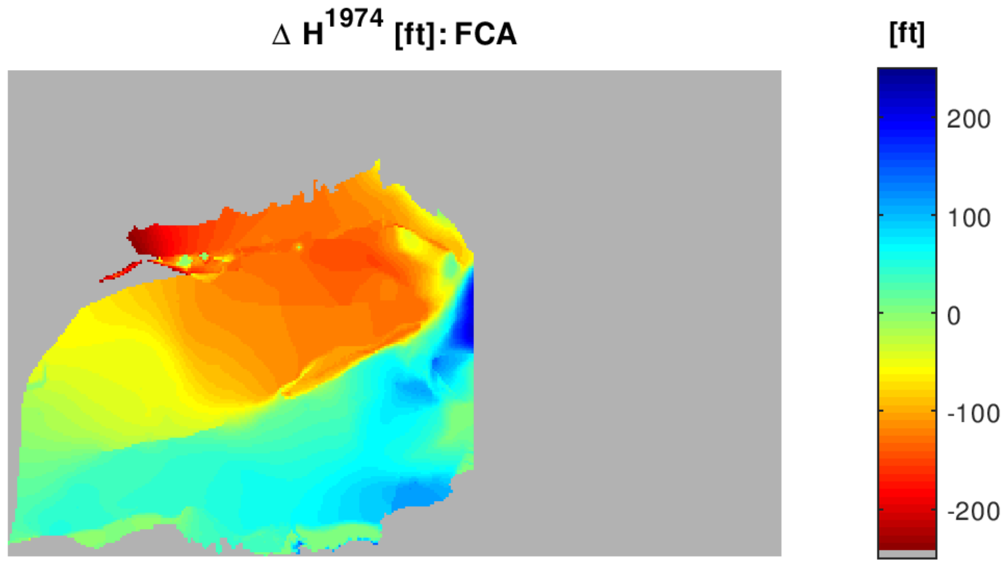

Figure 7: Difference in groundwater elevation in the FCA between Dec 1974 and Dec 2069.

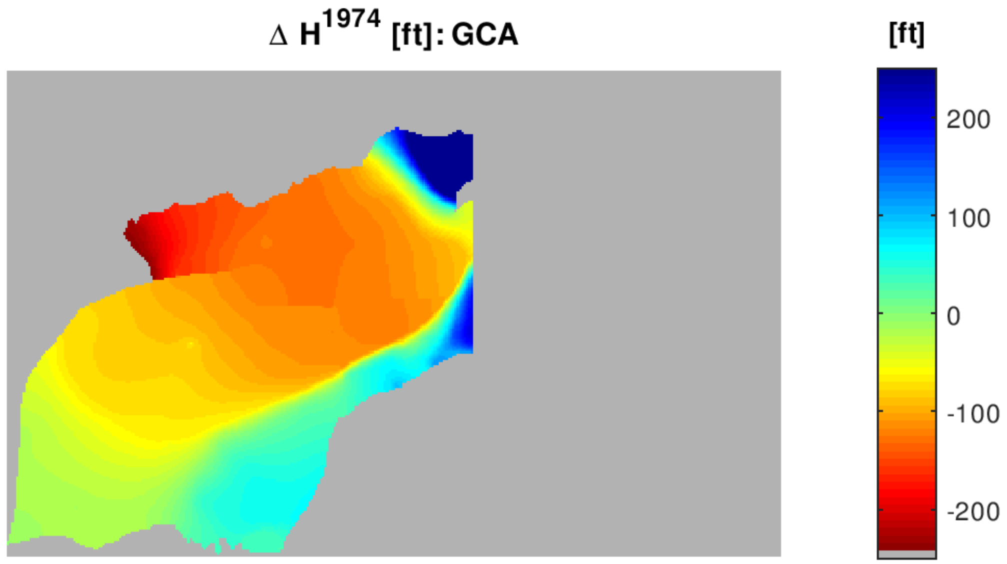

Figure 8: Difference in groundwater elevations in the GCA between Dec 1974 and Dec 2069.

Effects of Declining Water Levels on Aquifer Storage

Basin-wide declines in groundwater elevations indicate that storage is reduced between 2015 and 2069. Table 1 shows the change in storage from Dec 2015 conditions for Dec 1974 and Dec 2069. This comparison shows that storage increased across the entire model by nearly 120,000 AF from Dec 1974 to Dec 2015. The largest increases occurred in the USP, which benefitted from increased discharge to the Arroyo by the City of Simi Valley. In the FCA, storage increased by over 45,000 AF. Changes in the Grimes and Epworth gravels was negligible during this time period.

Results from the storage analysis show that management strategies implemented in the Future Baseline Scenario more than offset the increase in storage that occurred between 1974 and 2015. Under the Future Baseline Scenario conditions, more than 200,000 AF of storage is lost during the 50-year simulation. This corresponds to an 8% loss in the total volume of water in storage based on simulated Dec 2015 water levels. Table 1 shows that largest losses occur in the USP, where storage decreased by nearly 90,000 AF. In the FCA, storage decreased by nearly 80,000 AF. The fact that the greatest losses occur in the uppermost formation, the USP which receives most of the recharge to the ELPMA, emphasizes that the Future Baseline production rate exceeds the recharge rate.

Table 1: Storage in Dec 1974 and Dec 2069 compared to storage in Dec 2015.

Change in Storage from Dec 2015 Conditions [AF]		
Aquifer Unit	Dec 1974	Dec 2069
Epworth Gravels	-318 (-2%)	-9,154 (-45%)
Shallow Aquifer	-26,377 (-59%)	-5605 (-12%)
USP	-47,562 (-6%)	-89,623 (-11%)
FCA	-45,120 (-5%)	-78,977 (-8%)
GCA	+266 (0.04%)	-26,095 (-4%)
Total	***-119,111 (-5%)***	***-209,454 (-8%)***

Local Reductions in Aquifer Storage

Global reduction in aquifer storage suggests that basin management under the Future Baseline conditions will lead to a reduction in storage below 1974 levels across the ELPMA. However, the complex geologic structure of the FCA suggests that localized regions of ELPMA may be affected differently as groundwater elevations decline. Figure 9 shows that the FCA drops to its lowest elevations in the southwestern portion of the domain and along the major axes of the Las Posas and Moorpark synclines. In these synclines, the top surface of the Fox plunges to an elevation of approximately -430 ft. msl, which is nearly 900 feet lower than the high-point of the Moorpark Anticline which divides these two synclinal structures. Along the outcrop of the Fox Canyon aquifer (the northern extent of the model layer) the top elevation of the

FCA rises to an elevation greater than 1500 ft. msl, and south of the Arroyo Simi/Arroyo Las Posas, the top elevation of the FCA rises to approximately 1000 ft. msl.

Variations in the top elevation of the FCA lead to different aquifer conditions across East Las Posas. To quantitatively isolate regions where unconfined conditions occur in Dec 2015, we generated a map with

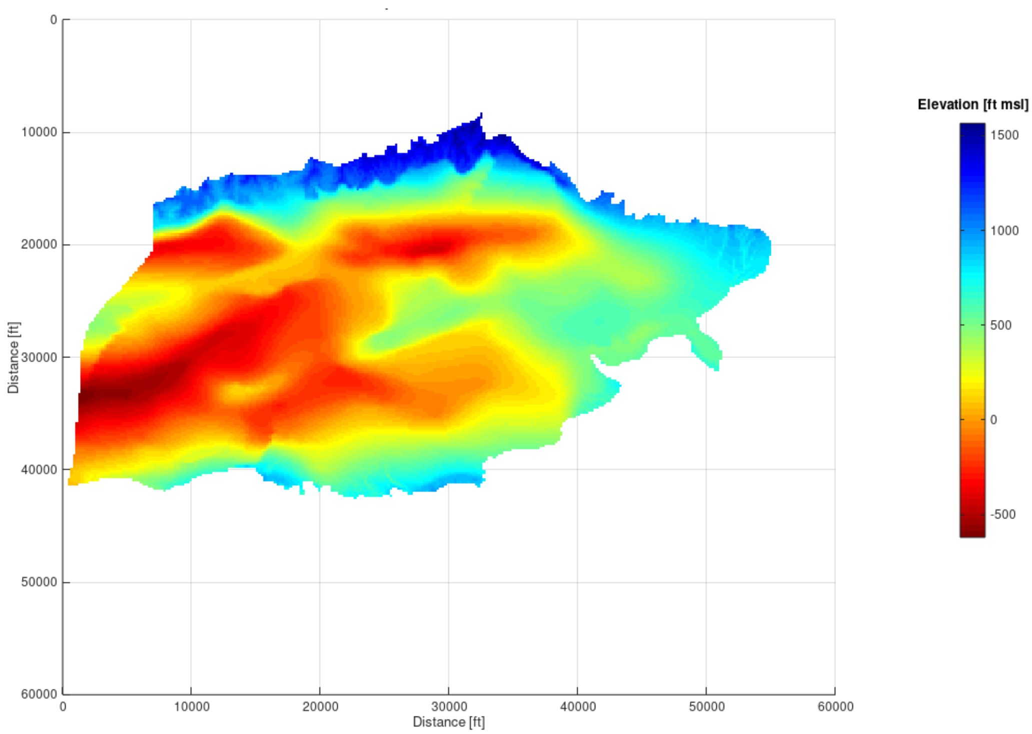

Figure 7: Elevation of the Top of the FCA as represented in the CMWD numerical model

8 zones of aquifer conditions across ELPMA (see Figure 10). A description of each zone by geographic location and aquifer condition is presented in Table 2. Figure 10 shows that confined aquifer conditions persist along the major axes of the Las Posas and Moorpark synclines (Zone D_n and D_s) in Dec 2015. Along the base of the South Mountain and Oak Ridge Mountains (Zone A), the ridge of the Moorpark Anticline (Zone B), south of the Arroyo (Zone C), and along the Long Canyon Anticline (Zone E), the FCA occurs under unconfined conditions. Because the specific yield is up to four orders-of-magnitude larger than specific storage, groundwater elevation declines in unconfined regions of the FCA may lead to larger reductions in storage when compared to zones that are confined.

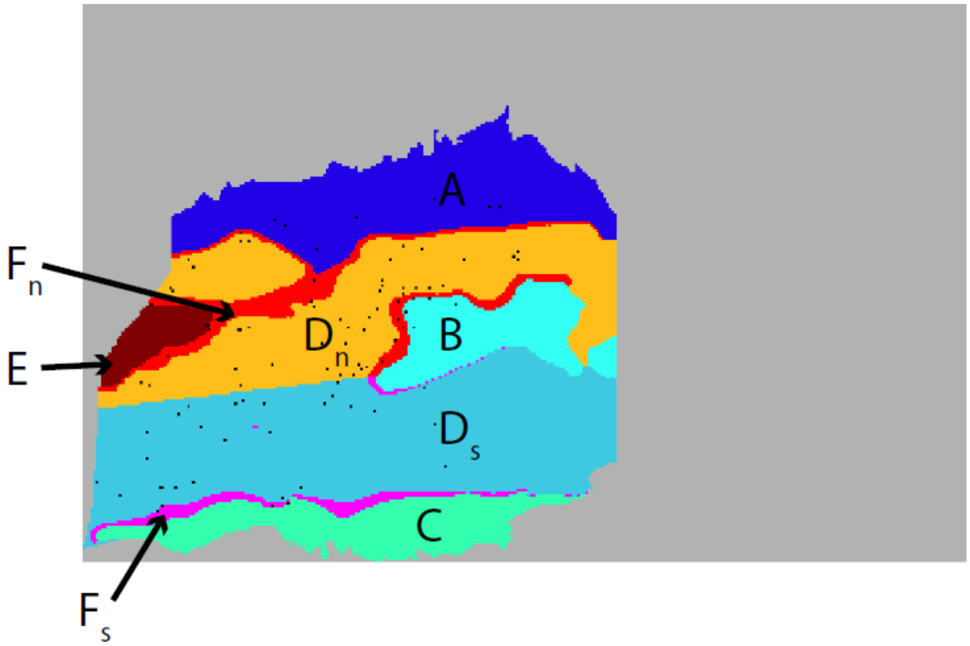

Figure 8: Zone Map that defines aquifer conditions based on geographic location across the ELPMA. Black dots indicate the location of specified flux boundary cells in the Fox Canyon Aquifer.

Table 2: Description of Geographic Locations and Dec 2015 Aquifer Conditions within each of the Zones Identified in Figure 10

Zone Indicator	Geographic Location	Aquifer Condition in Dec 2015
A	South Mountain and Oak Ridge Mountains	Unconfined
B	Ridge of the Moorpark Anticline	Unconfined
C	South of Arroyo Simi/Arroyo Las Posas	Unconfined
Dn	Along the axis of the Las Posas Syncline; north of the Moorpark Anticline	Confined
Ds	Along the axis of the Moorpark syncline; south of the Moorpark anticline	Confined
E	Long Canyon Anticline	Unconfined
Fn	Transition between A, B, E, and Dn	Confined (becomes unconfined by Dec 2069)
Fs	Transition between B, C, and Ds	Confined (becomes unconfined by Dec 2069)

To quantify the impact that localized differences in aquifer conditions have on storage losses, we segregated storage estimates in the FCA by the Zones specified in Table 2 and shown in Figure 10. Results from the Future Baseline Scenario show that storage losses in the FCA are largest in Zone A: declining water levels in this region led to a 17,600 AF reduction in storage, which is over 30% of the total volume stored in the region in Dec 2015. Aquifer responses are similar along the Moorpark Anticline (Zone B), where 16,000 AF of storage was lost during the 50-year future simulation. Groundwater elevation declines led to a 9300 AF reduction in confined storage north of the Moorpark anticline (zone D_n and F_n), and 7900 AF of confined storage south of the anticline (zone D_s and F_s).

Declining groundwater elevations in the FCA led to a transition from confined to unconfined conditions along the fringes of the FCA (F_n and F_s in Figure 10). This transition corresponded to 9000 AF of lost storage in the north, and 3700 AF of lost storage in the southern portion of ELPMA. Importantly, these declining groundwater elevations increased the unconfined area of the FCA by 6% (1720 acres); by the end of the Dec 2069 simulation, 38% of the FCA occurred under unconfined conditions

Table 3: Local Storage Losses across the FCA

Projected Impacts in the FCA by Dec 2069 under the Baseline Future Scenario Simulations (ignoring the Eastern portion of the model where there are no wells)							
Zone	Fraction of the FCA	Average head decline [ft] (+/- 1 stdev)	Area of the FCA that is unconfined in this zone [Acres]	Loss of Confined Storage [AF]	Loss of Confined Storage [% of 2015]	Total Loss of Storage [AF]	Total Loss of Storage [% of 2015]
A	15%	83 +/- 41	4242 (4620 cells)	–	–	17623	36%
B	7%	44 +/- 45	1814 (1975 cells)	–	–	8715	32%
C	8%	51 +/- 35	2266 (2468 cells)	–	–	16256	33%
Dn	20%	78+/-39	–	8120	29%	8120	3%
Ds	29%	57+/-37	–	7618	19%	7618	2%
E	2%	90 +/- 12	602 (656 cells)	–	–	7792	25%
Fn	4%	94 +/- 26	1228 (1337 cells)	1178	100%	9097	12%
Fs	2%	77 +/- 27	492 (536 cells)	309	100%	3756	13%
TOTAL			**10644 (11592 Cells)**	**17225**	**24%**	**78977**	**8%**

Table 4: Local Storage Losses across the USP

Projected Impacts in the USP by Dec 2069 under the Baseline Future Scenario Simulations in the USP (ignoring the Eastern portion of the model where there are no wells)							
Zone	Fraction of the USP (Layer 2)	Average head decline [ft] (+/- 1 stdev)	Area of the FCA that is unconfined in this zone [Acres]	Loss of Confined Storage [AF]	Loss of Confined Storage [% of 2015]	Total Loss of Storage [AF]	Total Loss of Storage [% of 2015]
A	16%	56 +/- 52	3286 (3579 cells)	0	–	1099	64%
B	7%	18 +/- 58	1814 (1975 cells)	0	–	408	10%
C	8%	47 +/- 37	1899 (2068 cells)	0	–	6	93%
Dn	21%	29 +/- 48	5559 (6054 cells)	2102	26%	39666	14%
Ds	29%	28 +/- 37	6142 (6689 cells)	3738	11%	35776	8%
E	2%	51 +/- 48	602 (656 cells)	0	–	969	33%
Fn	5%	35 +/- 37	1228 (1337 cells)	0	–	10126	35%
Fs	2%	74 +/- 36	492 (536 cells)	4	100%	1572	69%
TOTAL			**21022**	**5844**	**15%**	**89622**	**11%**

Effects of Declining Groundwater Elevations on Well Yields

The CMWD numerical model represented production within the FCA in the Future Baseline Scenario using 98 specified flux boundary cells. Of these 98 cells, 22 were in regions of the FCA that were unconfined by Dec 2069. Results from the Future Baseline Scenario simulation (using $\Phi = 0.99$) show that total production losses across the basin were relatively small (3%, 481 AF); however, reduction in well yields exceed 50% in local regions of the FCA. Losses were largest in Zone A (base of South Mountain and Oak Ridge Mountains) and Zone B (along the Moorpark Anticline). In Zone A, well yields were impacted by 56%, and in Zone B, well yields declined by nearly 80% (approximately 300AF).

Table 5: Impact of Declining Groundwater Elevations on Well Yields in the FCA

Projected Impacts by Dec 2069 under the Baseline Future Scenario Simulations (ignoring the Eastern portion of the model)							
Zone	Total area of zone [acres]	Fraction of the FCA	# of Wells in the Zone	# of Wells impacted	Specified Production from Zone in 2070 [AF]	Actual Production from Zone in 2070 [AF]	Loss of Production [%]
A	4166	15%	7	7	102	45	56%
B	1944	7%	5	1	394	88	78%
C	2222	8%	1	1	36	10	71%
Dn	5555	20%	43	0	6713	6713	0%
Ds	8055	29%	27	2	7123	7122	0%
E	556	2%	2	2	926	852	8%
Fn	1111	4%	11	7	12834	1265	1%
Fs	556	2%	2	2	358	353	1%
TOTAL			**98**	**22**	**16936**	**16448**	**3%**

Estimating Reduced Recharge Potential in the FCA

The progressive drying of the FCA may lead to the development of an unsaturated zone that limits leakage from the USP into the Fox. To quantify the potential impact of unsaturated flow on recharge to the Fox, we developed an unsaturated flow model using the USGS software VS2DT. Using average values for the hydraulic parameters in the CMWD model for the USP, Clay Marker Bed, and Fox Canyon Aquifer, we designed a heterogeneous flow domain that mimicked the representative stratigraphic layering in ELPMA. We first set the initial saturation of the upper model layer (USP), Clay Marker bed, and FCA equal to 1 and applied a constant head at the top of the USP to force flow through the domain. We estimated the recharge rate into the Fox under this fully-saturated condition by measuring the flux leaving the confining bed.

After running this simulation, we introduced an unsaturated zone that separated the fully saturated USP and clay marker bed from the underlying water table in the Fox. Keeping boundary conditions the same as the fully-saturated simulations, we measured the flux of water entering the water table in the Fox. Recharge rates to the Fox under these partially saturated conditions were 10% lower than the rates estimated using the VS2DT results from the fully saturated model. To estimate the potential impact that this would have in the CMWD numerical model, we took the average MODFLOW-calculated recharge rate from the USP into the Fox and reduced it by 10% in each cell of the FCA that occurred under unconfined conditions.

In Zone A, the largest area of unconfined FCA, the potential loss of recharge due to unsaturated flow is approximately 275 AFY. Unconfined conditions in Zones B, C, and E may lead to an additional loss in recharge of 358 AFY, and the newly created unconfined conditions in Zones F_n and F_s may cause 36 AFY loss in recharge. Because the CMWD numerical model does not incorporate a mechanistic expression for recharge reductions that occur due to unsaturated conditions in deeper aquifer units, the model may be slightly underestimating the total loss in storage across the ELPMA.

Summary

We used results from the CMWD numerical model, run under the Future Baseline Scenario conditions, to quantify changes in storage, recharge potential, and well yields from Dec 2015 conditions. The results of our analysis show that decreased discharges to the Arroyo and continued production at 2015-17 average rates may lead to approximately 90,000 AF of lost storage in the USP by Dec 2069. Decreased storage and declining heads in the USP limit recharge into the Fox, which is the principal production unit within ELPMA. Under the Future Baseline Scenario conditions, results from the CMWD numerical model indicate the potential loss of 79,000 AF of water from the FCA. The combined storage losses across the ELPMA exceed 200,000AF by Dec 2069, which is an 8% reduction in storage from Dec 2015 conditions.

Notably, management under the Future Baseline Scenario conditions leads to a 6% increase in the area of the FCA that occurs under unconfined conditions (Local head < Top elevation of the FCA). By Dec 2069, the model results indicate that over 10,000 acres (or 38% of the Fox) will be unconfined. Impacts to basin-wide recharge and well yields are small. However, recharge and production in the northern extent of ELPMA, and along the Moorpark anticline, may be impacted by declining heads and a progressive transition to unconfined conditions in the Fox.

References

Konikow, L.F., Hornberger, G.Z., Halford, K.J., and Hanson, R.T., 2009, Revised multi-node well (MNW2) package for MODFLOW ground-water flow model: U.S. Geological Survey Techniques and Methods 6–A30, 67 p.

Niswonger, R.G., Panday, Sorab, and Ibaraki, Motomu, 2011, MODFLOW-NWT, A Newton formulation for MODFLOW-2005: U.S. Geological Survey Techniques and Methods 6–A37, 44 p.

Fetter, C.W., 2001, *Applied Hydrogeology,* Upper Saddle River, New Jersey: Prentice-Hall.